

<https://doi.org/10.17221/76/2025-CJGPB>

# Seasonal and microclimate-responsive expression of *VRN-A1* and *VRN-B1* in wheat under field conditions

NICOLE FRANTOVÁ<sup>1\*</sup>, ILJA TOM PRÁŠIL<sup>2</sup>, LUDMILA HOLKOVÁ<sup>1</sup>

<sup>1</sup>Department of Crop Science, Breeding and Plant Protection, Faculty of AgriSciences, Mendel University in Brno, Brno, Czech Republic

<sup>2</sup>Plant Stress Biology and Biotechnology, Czech Agrifood Research Center, Praha, Czech Republic

\*Corresponding author: [xfrantov@mendelu.cz](mailto:xfrantov@mendelu.cz)

**Citation:** Frantová N., Prášil I.T., Holková L. (2026): Seasonal and microclimate-responsive expression of *VRN-A1* and *VRN-B1* in wheat under field conditions. Czech J. Genet. Plant Breed., 62: 53–63.

**Abstract:** The need of vernalisation, controlled by the gene *VRN-1*, impacts wheat adaptation and yield stability, yet field evidence on the plasticity of *VRN-1* homoeologs expression is limited. We quantified *VRN-1* homoeolog dynamics across two sites and two seasons in seven cultivars, by sampling their apex and leaf. *VRN-A1* varied with genotype ( $P < 0.001^{***}$ ), tissue (apex > leaf;  $P < 0.001^{***}$ ), apex development ( $P < 0.001^{***}$ ), day length ( $P < 0.001^{***}$ ), and to a lesser extent, on short-term freezing exposure, quantified as a 5-day freezing-degree sum (FDS;  $P = 0.019^*$ ). Photoperiod class (*Ppd-D1a* vs *Ppd-D1b*) added an additional effect ( $P = 0.001^{***}$ ). *VRN-B1* showed strong genotype effects ( $P < 0.001^{***}$ ), a modest effect of site on its expression ( $P = 0.025^*$ ), and pronounced associations with microclimate variables (day length, thermal sums, freezing exposure; all  $P < 0.001^{***}$ ). Directionally, *Ppd-D1a* backgrounds tended to advance the development while showing earlier apex *VRN-A1* peaks. Overall, *VRN-A1* expression mainly reflected developmental stage and seasonal forcing, whereas *VRN-B1* might be more microclimate-responsive, indicating complementary roles for timing and stress-response plasticity. To isolate causal effects and to further explain these dynamics, targeted sequencing and tests in near-isogenic lines will be needed in future work.

**Keywords:** field-based gene expression; flowering time adaptation; photoperiod sensitivity; *Triticum aestivum*; *VRN-1* homoeologs

Control of flowering time is a key determinant of wheat adaptation and yield stability, as the transitions from stem elongation to heading and maturity determine how efficiently plants convert resources into grain (Chen et al. 2010; Langer et al. 2014). These developmental phase changes are regulated by genetic pathways that sense temperature (vernalisation) and day length (photoperiod) and coordinate developmental rate within the cropping season (Snape et al. 2001; Shcherban et al. 2015). Vernalisation

requirements vary among genotypes and are most efficiently fulfilled by prolonged exposure to 0–10 °C, with strongly reduced effects above 11 °C (Brooking 1996; Curtis et al. 2002). In European winter cultivars, this corresponds to 5–13 weeks of cold exposure (Košner & Pánková 2002; Petr & Hnilička, 2002). Allelic composition of the *VRN-1* homoeologs largely determines this requirement, with dominant alleles shortening and recessive haplotypes extending it (Yan et al. 2004; Kamran et al. 2014).

Supported by the National Agency for Agricultural Research (NAZV), Ministry of Agriculture of the Czech Republic (Project QL24010142), and by institutional funding from the Ministry of Agriculture of the Czech Republic (Project MZE-RO0425).

© The authors. This work is licensed under a Creative Commons Attribution-NonCommercial 4.0 International (CC BY-NC 4.0).

The central role in the vernalisation pathway has *VRN-1*, a MADS-box transcription factor with three homoeologous copies in hexaploid wheat: *VRN-A1*, *VRN-B1* and *VRN-D1* on chromosome 5 (Galiba et al. 1995; Kiss et al. 2014). Winter habit typically carries recessive *vrn-A1/vrn-B1/vrn-D1* (vernalisation required), whereas the presence of  $\geq 1$  dominant *Vrn-1* allele confers a spring habit (no vernalisation required). To avoid ambiguity, we define ‘facultative’ as a phenotypic subset of spring lines that do not require vernalisation yet overwinter reliably when autumn-sown. The homoeologs differ in their effect size on earliness ( $A1 > B1 > D1$ ), corresponding to heading-time contrasts observed in the field (Stelmakh 1992; Zhang et al. 2008, 2022).

*VRN-1* activity is embedded in a wider regulatory network. *VRN2* encodes CCT-domain zinc-finger transcriptional repressors of flowering that are down-regulated by prolonged cold (vernalisation) (Yan et al. 2004; Distelfeld et al. 2009). Conversely, *VRN-3/FT1* integrates vernalisation and photoperiod signals from leaves to the shoot apex and promotes *VRN-1* transcription, assisted by 14-3-3 and bZIP proteins (Yan et al. 2006; Li & Dubcovsky 2008; Li et al. 2015; Sehgal et al. 2023). In turn, *VRN-1* down-regulates *VRN-2* in leaves, completing a regulatory feedback loop (Hemming et al. 2008; Chen & Dubcovsky 2012). Epigenetic modifications, particularly within intron 1, provide a “memory” of cold exposure, referring to vernalisation-associated chromatin remodelling at *VRN-1*, such as DNA-methylation changes, while

a *VRN-1*-derived long non-coding RNA enhances promoter activation (Khan et al. 2013; Oliver et al. 2009; Xu & Chong 2018; Xu et al. 2021).

This architecture functions within broader transcription-factor families: MADS-box proteins (*VRN-1*) provide meristem identity, zinc-finger/CCT proteins (*VRN-2*) enforce seasonal repression, and *VRN-3* transmits environmental cues to transcriptional change (Takatsuji 1998; Smaczniak et al. 2012).

We hypothesised that microclimate affects *VRN-1* homoeolog expression in the field, with tissue specificity and *Ppd-D1* alleles further shifting expression level and timing.

## MATERIAL AND METHODS

**Plant material.** Seven bread wheat cultivars were studied: six winter types (Balitus, Bohemia, IS Conditor, RGT Sacramento, Tobak, Tonnage) and one facultative type (Tybalt). Basic characteristics (origin, earliness, vernalisation requirement, and freezing tolerance, LT50) are summarised in Table 1. (Frantová 2024). Seeds for genetic analyses were provided by the Gene Bank, Czech Agrifood Research Center (Prague-Ruzyně); seeds for field trials (commercial cultivars) were supplied by a seed company. For each cultivar we also list the *VRN-1* homeolog combination (*VRN-A1/VRN-B1/VRN-D1*) and the *Ppd-D1* allele (Frantová 2024). *Ppd-D1* has the strongest effect on photoperiod in hexaploid wheat (Beales et al. 2007).

Table 1. Specifics about the chosen varieties

Variety	Origin	Earliness	Vernalisation requirements (weeks)	Freezing tolerance (LT50) (°C)	<i>VRN-1/Ppd-D1</i> allelic profile	Photoperiod sensitivity
Balitus	Austria	very early	long $\geq 7$	-16.0	<i>vrn-A1/vrn-B1/vrn-D1/Ppd-D1a</i>	insensitive
Bohemia	Czech Republic	very early	long $\geq 7$	-18.0	<i>vrn-A1/vrn-B1/vrn-D1/Ppd-D1a</i>	insensitive
IS Conditor	Slovak Republic	moderately early	medium 4–6	-13.5	<i>vrn-A1/vrn-B1/vrn-D1/ppd-D1b</i>	sensitive
RGT Sacramento	France	moderately early	medium 4–6	-13.5	<i>vrn-A1/vrn-B1/vrn-D1/Ppd-D1a</i>	insensitive
Tobak	Germany	semi-late	short 3–4	-14.5	<i>vrn-A1/vrn-B1/vrn-D1/ppd-D1b</i>	sensitive
Tonnage	Denmark	semi-late	short 3–4	-15.0	<i>vrn-A1/vrn-B1/vrn-D1/ppd-D1b</i>	sensitive
Tybalt	Netherlands	semi-late	none	-13.5	<i>vrn-A1/vrn-B1/Vrn-D1/ppd-D1b</i>	sensitive

<https://doi.org/10.17221/76/2025-CJGPB>

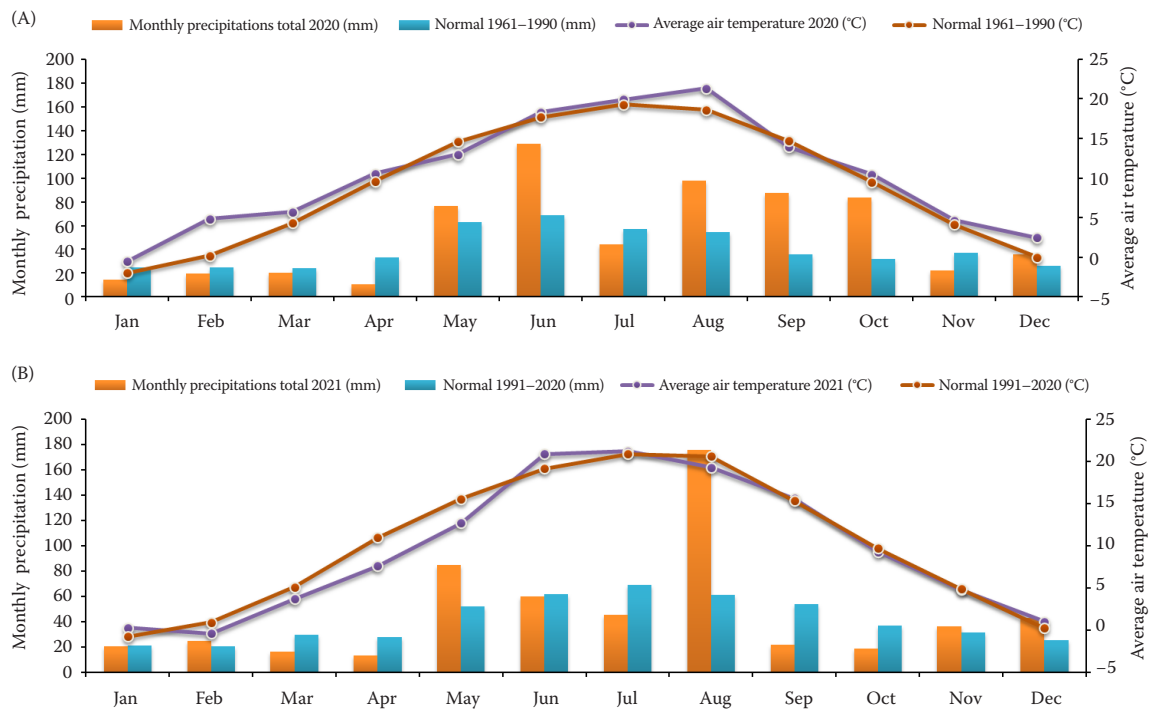


Figure 1. Monthly precipitation totals and mean air temperature for the study area in (A) 2020 and (B) 2021

We use the standard *VRN-1* nomenclature in which *Vrn-A1* denotes a dominant spring-like allele linked to intron-1/promoter deletions (Fu et al. 2005).

**Field sites, climatic conditions, and crop management.** The sites differed markedly in edaphic conditions. Site A (N 49°1'22.246", E 16°37'2.896", Nosislav, South Moravia, Czech Republic) had a finer texture with a higher clay fraction and a shallow water table (mean depths 1.35 m in 2020, 1.05 m in 2021), whereas Site B (N 49°0'45.941", E 16°33'47.083", Žabčice, South Moravia, Czech Republic) was sand-rich/coarser with a deep water table (16–18 m). Monthly precipitation and 2-m air temperature were obtained from the on-site station (Figure 1). In 2020, an early warm anomaly in February was followed by colder conditions in March and then a gradual temperature increase, whereas the 2021 season remained generally colder, with February also below the long-term normal and no comparable early warming.

The plots were arranged as randomised complete blocks (three replicates at site A, four at site B); the net plot area was 10.3 m<sup>2</sup> (7.3 × 1.37 m). Sowing occurred in early October each season (site A: 15. 10. 2019 and 8. 10. 2020; site B: 8. 10. 2019 and 7. 10. 2020). Fertilisation regimes followed standard station practice. Further information can be found in Frantová (2024).

### Phenology scaling and environmental variables.

Development of the main-stem shoot apex was recorded and measured under a stereomicroscope with the Waddington scale (WS; 0–10 with decimal subdivisions, Waddington et al. 1983). Sampling frequency increased from winter to spring as development accelerated (Table 2).

From the available environmental cues, we selected four for analysis: daylength; growing degree days accumulated from the first November observation to each subsequent sampling (25 Nov 2019; 12 Nov 2020); the low-temperature sum over the same period; and a short-term freezing-degree sum computed from the 5-day 07:00–07:00 window preceding sampling. All temperature metrics were derived from above-ground, near-surface air temperature.

Daylength (DL) was computed as the interval between apparent sunrise and apparent sunset for the study coordinates on each sampling date, using the NOAA Global Monitoring Laboratory Solar Calculator (NOAA 2025).

Above-ground temperature was recorded by the sensors at each site (TepUni temperature sensor, AMET Velké Bílovice). Growing degree days (GDD) expressed in hours quantify thermal time above 5 °C (baseline), computed from the first November sampling as:

$$\text{GDD}_5^h = \sum_{\text{hours}} \max(0, T_{\text{hours}} - 5 \text{ } ^\circ\text{C}) \text{ (} ^\circ\text{C}\cdot\text{h)} \quad (1)$$

Cold exposure (low temperature sum, LTS) was computed from daily mean temperatures using a  $\leq 5 \text{ } ^\circ\text{C}$  inclusion rule: values  $> 5 \text{ } ^\circ\text{C}$  contribute 0; values  $\leq 5 \text{ } ^\circ\text{C}$  contribute their magnitude, negatives values turned into positive. To quantify recent sub-zero exposure (freezing-degree sum, FDS), we computed a 5-day freezing-degree sum from 15-min air-temperature series using a  $0 \text{ } ^\circ\text{C}$  base. For each sampling date  $t_s$ , we integrated from 07:00 on the sampling day back 5 days. This window was chosen because tissue was sampled at 08:00–09:00, ensuring only pre-sampling exposure contributes.

**Transcriptome analysis.** For expression analyses, two shoot apices with subtending stems and the 1<sup>st</sup>–3<sup>rd</sup> youngest and healthy-looking leaves of the main stem were sampled with two biological replicates. Each biological replicate was a pooled sample (two leaves pooled = one leaf sample; two apices pooled = one apex sample). Field sampling on each date was conducted between 08:00 and 09:00 local time (CET/CEST) to minimise diurnal variation in transcript levels. Material was snap-frozen in liquid  $\text{N}_2$  in the field and stored at  $-80 \text{ } ^\circ\text{C}$  until RNA extraction. Total RNA was extracted using the RNeasy Plant Mini Kit (QIAGEN; spin-column protocol; 80  $\mu\text{L}$  RNase-free water elution). Residual genomic DNA was removed with TURBO DNA-free<sup>TM</sup> (Invitrogen), the input was 3 000 ng of RNA per 20  $\mu\text{L}$  of each sample. First-strand cDNA was synthesised using the RevertAid First Strand cDNA Synthesis Kit (Thermo Fisher Scientific).

**Real-time PCR analysis.** Quantitative PCR was performed with SYBR Green chemistry using Light-Cycler<sup>®</sup> 480 SYBR Green I Master (Roche) on a Bio-

Rad iQ<sup>TM</sup>5 (96-well plates; 20  $\mu\text{L}$  reactions, 1  $\mu\text{L}$  cDNA; 40 cycles, kit-recommended cycling). Primer sequences and optimised annealing conditions were as follows: *ACTIN* (Aslam et al. 2017; annealing  $60 \text{ } ^\circ\text{C}$  for 15 s), *VRN-A1* (Loukoianov et al. 2005; annealing  $64 \text{ } ^\circ\text{C}$  for 15 s) and *VRN-B1* (Frantová 2024; annealing  $64 \text{ } ^\circ\text{C}$  for 15 s). *ACTIN* served as the reference gene, samples were diluted 10 $\times$ , and normalised relative expression was calculated according to Pfaffl (2001). Melt-curve analysis confirmed single specific amplicons, and amplification efficiencies ranged from 88% to 100% ( $E = 1.88\text{--}2.00$ ).

**Statistical analysis.** Preliminary linear-model/ANOVA fits to the qPCR expression data were used to check assumptions. For *VRN-A1*, residuals showed clear deviations from normality and strong heteroscedasticity, and expression was analysed using a generalised linear model (GLM) with a Gamma distribution and log link. In contrast, *VRN-B1* expression approximately satisfied normality and homoscedasticity, and was therefore analysed using a Gaussian GLM with an identity link. Fixed factors were genotype, tissue and site; covariates were apex developmental stage (Waddington scale) and microclimate variables (FDS, LTS, GDD, DL), including their interactions. Significance of effects was assessed with Type III Wald  $\chi^2$  tests ( $\alpha = 0.05$ ); we report generalised partial  $\eta^2$  as an effect-size measure and marginal  $R^2$  as an indicator of model fit. Because of CPU/memory limits, the effect of photoperiod-sensitivity class (*Ppd-D1*) was tested in a separate reduced model for each gene. GLM analyses were performed in jamovi Ver. 2.7 (the jamovi project, Australia) based on the R environment. Bivariate associations between expression, phenology and environmental variables were evaluated using Spearman's rank correlation

Table 2. Sampling dates with daylength and 5-day freezing-degree sum

Growing season	Day length (h)	FDS (h of $< 5 \text{ } ^\circ\text{C}$ )		Growing season	Day length (h)	FDS (h of $< 5 \text{ } ^\circ\text{C}$ )	
		site A	site B			site A	site B
2019–2020	both sites			2020/2021	both sites		
8.1.2020	8.5	251.8	184.0	4. 12. 2020	8.6	104.5	84.0
12.2.2020	10.0	76.3	39.3	28. 1. 2021	9.2	72.8	51.0
10.3.2020*	11.6	35.0	25.8	25. 2. 2021	10.8	17.5	6.3
18.3.2020	12.1	93.5	50.0	18. 3. 2021	12.1	62.0	13.3
1.4.2020	12.9	141.0	133.5	30. 3. 2021*	12.8	13.8	0
15.4.2020	13.7	46.8	15.8	12. 4. 2021	13.6	85.0	39.0
28.4.2020	14.5	11.5	0	23. 4. 2021	14.2	12.5	0.3
				28. 4. 2021	14.5	10.5	0

FDS – freezing-degree sum; \*denotes the Waddington W2.0 (double ridge) apex stage, the onset of spikelet initiation

<https://doi.org/10.17221/76/2025-CJGPB>

(two-tailed,  $P < 0.05$ ) in XLSTAT (Excel add-in; Lumivero, USA), with Excel used for data handling and heat-map graphics.

## RESULTS AND DISCUSSION

***VRN-A1* transcripts seem lower in a facultative cultivar and earlier in *Ppd-D1a* genotypes.** Across seasons and tissues, the winter cultivars showed cold-responsive *VRN-A1* induction under field conditions (Figure 2), with transcript levels generally higher in the apex than in leaves. In the relatively mild 2020 season, characterised by a warm February followed by colder spells in March, *Ppd-D1a* carriers (Balitus, Bohemia) tended to show earlier and

stronger apex induction, whereas *ppd-D1b* carriers more often displayed slower, delayed peaks. In the colder 2021 season, with February temperatures also below the long-term normal, *VRN-A1* peaks were generally shifted later and were weaker, especially in photoperiod-sensitive (*ppd-D1b*) genotypes. This pattern is consistent with the view that “insensitive” *Ppd-D1a* alleles retain some photoperiod responsiveness but favour earlier or stronger *VRN-A1* activation when vernalisation is partially satisfied (Slafer et al. 2023). The facultative cultivar Tybalt maintained low *VRN-A1* expression (often  $< 2.0$ ) in both years, in line with reports that facultative wheats require little or no vernalisation and therefore accumulate lower *VRN-1* under winter conditions (Pražil et al.

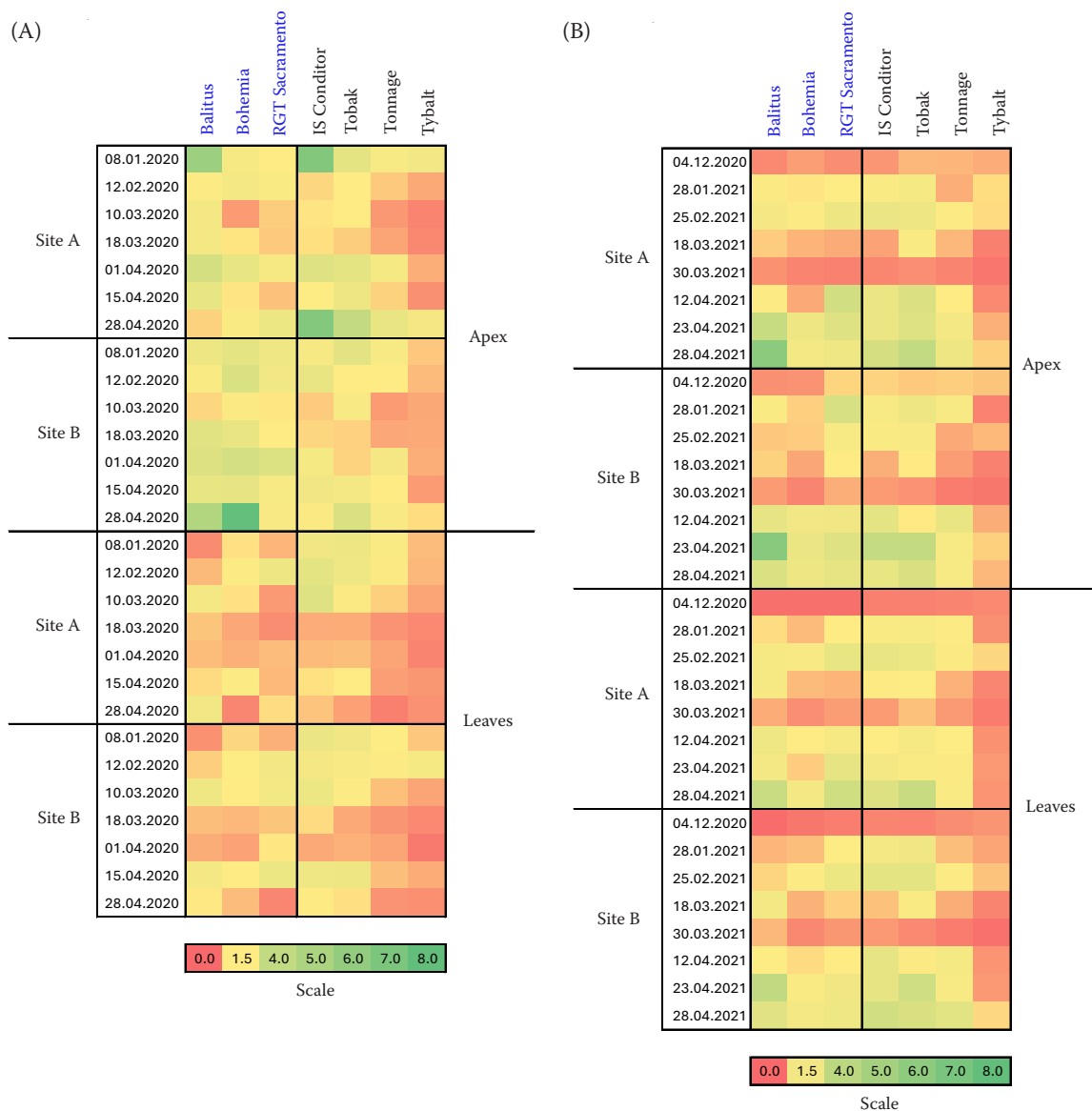


Figure 2 continues on the next page

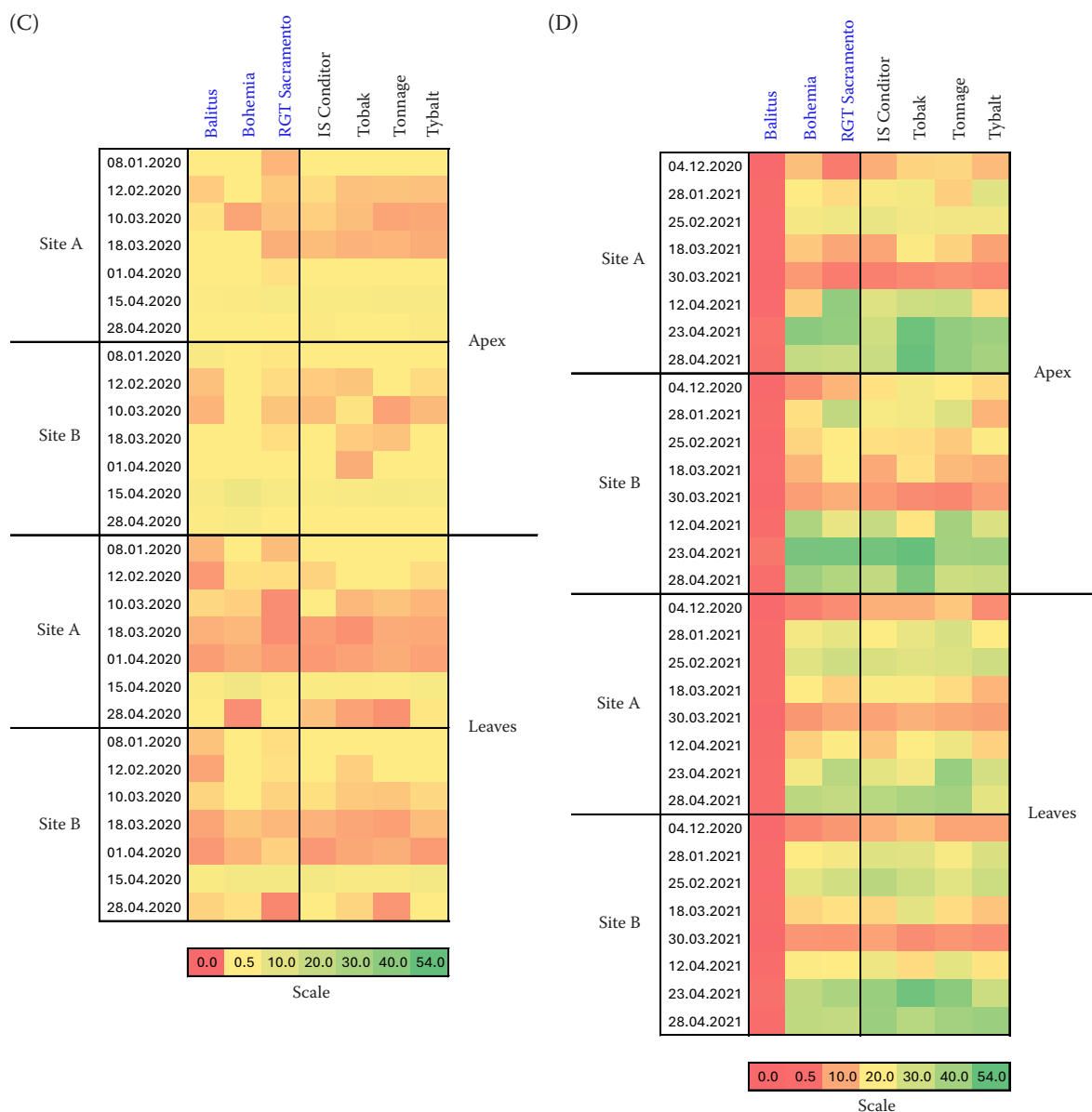


Figure 2. Heat maps of normalised relative expression (NRE): *VRN-A1* (A–B), *VRN-B1* (C–D) (two seasons × two sites × two tissues); blue labels indicate genotypes carrying the photoperiod-insensitive allele *Ppd-D1a*

2025). From an applied perspective, combining information on *VRN-A1* apex dynamics with *Ppd-D1* background and typical seasonal temperature patterns may help prioritise cultivars for late-autumn sowing (Wenda-Piesik et al. 2016).

***VRN-B1* appears more environmentally responsive than *VRN-A1*.** Compared with *VRN-A1*, *VRN-B1* expression was more variable and strongly season-dependent. In the milder winter of 2020, *VRN-B1* transcripts remained low across genotypes, whereas in the colder 2021 season they increased markedly, with pronounced April peaks in Tobak

and Tonnage while Balitus stayed low. Two non-exclusive mechanisms may underlie this pattern. First, allelic differences at *VRN-B1*. This gene shows extensive sequence diversity (promoter changes, intron-1 indels and several non-synonymous SNPs) and allele-dependent expression under controlled vernalisation, implying genotype-specific baselines and responsiveness (Strejčková et al. 2023).

Second, environmental dose and timing of cold. *VRN1* transcription in leaves is promoted by prolonged low temperatures and contributes to repression of *VRN-2*, so winter-to-winter differences in cold

<https://doi.org/10.17221/76/2025-CJGPB>

accumulation and fluctuation can shift expression amplitude or timing (Chen & Dubcovsky 2012). In 2021, intermittent warm spells followed by renewed cold likely reinforced vernalisation signalling and favoured stronger *VRN-B1* induction, while the milder 2020 season remained below this threshold. Tybalt, which showed weak *VRN-A1* but strong *VRN-B1* induction in 2021, further suggests partial functional compensation between homeologs, with *VRN-A1* more strongly promoted by genotype/development and *VRN-B1* acting as the more environmentally responsive copy in our field conditions.

**Photoperiod group and tissue shape *VRN-A1*.** Generalised linear models (Table 3) showed that

*VRN-A1* expression varied strongly with genotype ( $P < 0.001$ ;  $R^2 = 0.319$ ) and tissue, with consistently higher levels in the apex than in leaves ( $P < 0.001$ ). Apex developmental stage ( $P < 0.001$ ), day length (DL;  $P < 0.001$ ) and short-term freezing (FDS;  $P = 0.019$ ) were also significant predictors, whereas site and all tested interactions were not. The significant DL effect should not be read as a simple linear day-length response; it most likely reflects mediation by the photoperiod pathway, where *FT1* produced in leaves under long days (*Ppd-D1* dependent) forms an FT–14–3–3–FD complex that promotes *VRN-1* transcription in the apex. In a reduced model, photoperiod class (*Ppd-D1a* vs *ppd-D1b*) further modified *VRN-A1*

Table 3. Generalised linear models (GLMs) results for *VRN-A1* (Gamma–log) and *VRN-B1* (Gaussian–identity)

Gene		$\chi^2$	<i>df</i>	<i>P</i> -value	$\eta^2$	$R^2$	
<i>VRN-A1</i>	genotype	195.95	6	< 0.001***	$3.30 \times 10^{-1}$	0.319 ( $P < 0.001$ ***)	
	tissue	30.44	1	< 0.001***	$5.13 \times 10^{-2}$		
	site	1.58	1	0.209	$2.66 \times 10^{-3}$		
	apex development	31.54	1	< 0.001***	$5.31 \times 10^{-2}$		
	FDS	5.51	1	0.019*	$9.27 \times 10^{-3}$		
	LTS	1.01	1	0.316	$1.70 \times 10^{-3}$		
	GDD	0.27	1	0.607	$4.46 \times 10^{-4}$		
	DL	14.12	1	< 0.001***	$2.38 \times 10^{-2}$		
	genotype × tissue	7.73	6	0.258	$1.30 \times 10^{-2}$		
	genotype × site	4.54	6	0.605	$7.64 \times 10^{-3}$		
	tissue × site	0.08	1	0.780	$1.31 \times 10^{-4}$		
	genotype × tissue × site	4.94	6	0.552	$8.32 \times 10^{-3}$		
	photoperiod sensitivity	10.40	1	0.001***	$1.75 \times 10^{-2}$		0.012 ( $P < 0.001$ ***)
	<i>VRN-B1</i>	genotype	81.65	6	< 0.001***		$5.96 \times 10^{-5}$
tissue		0.74	1	0.390	$5.39 \times 10^{-6}$		
site		5.05	1	0.025*	$3.68 \times 10^{-5}$		
apex development		1.16	1	0.282	$8.43 \times 10^{-6}$		
FDS		26.97	1	< 0.001***	$1.97 \times 10^{-4}$		
LTS		23.00	1	< 0.001***	$1.68 \times 10^{-4}$		
GDD		37.49	1	< 0.001***	$2.74 \times 10^{-4}$		
DL		49.63	1	< 0.001***	$3.62 \times 10^{-4}$		
genotype × tissue		1.23	6	0.975	$9.01 \times 10^{-6}$		
genotype × site		1.58	6	0.954	$1.15 \times 10^{-5}$		
tissue × site		0.41	1	0.524	$2.97 \times 10^{-6}$		
genotype × tissue × site		1.24	6	0.975	$9.04 \times 10^{-6}$		
photoperiod sensitivity		17.60	1	< 0.001***	$1.28 \times 10^{-4}$	0.021 ( $P < 0.001$ ***)	

FDS – freezing-degree sum; LTS – low temperature sum; GDD – growing degree days; DL – daylength; *df* – degree of freedom;  $\eta^2$  – effect size (proportion of variability in the response explained by the factor)

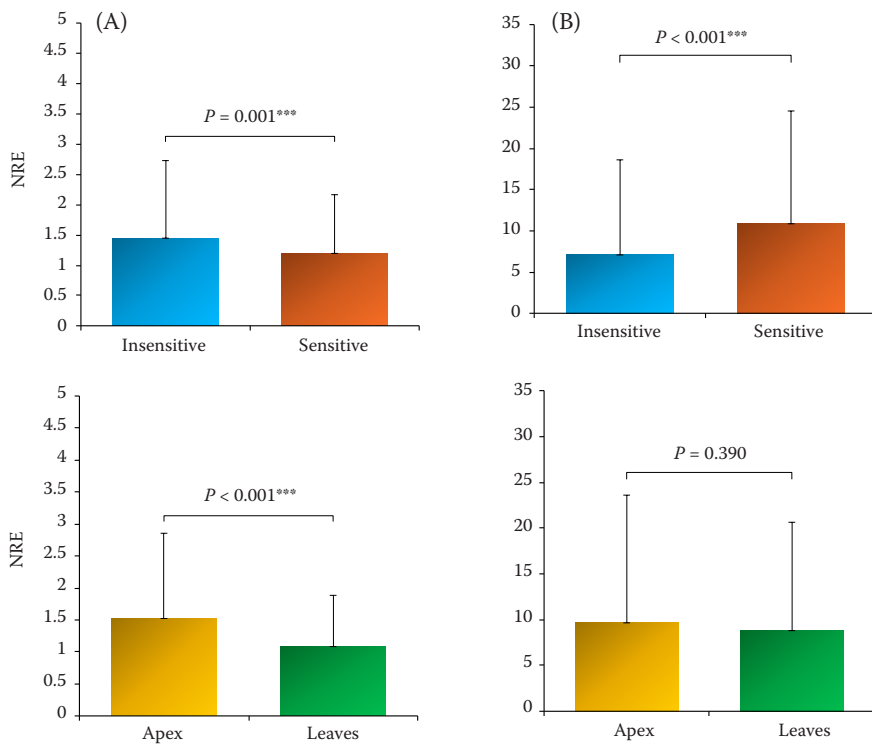


Figure 3. Normalised relative expression (NRE) by photoperiod type and tissue: *VRN-A1* (A), *VRN-B1* (B). Error bars represent standard deviation.

expression ( $P = 0.001$ ), with photoperiod-insensitive genotypes tending to reach higher apex transcript levels earlier in development. Together with the more environment-sensitive behaviour of *VRN-B1*, these results support *VRN-A1* as the primary, apex-localised homeolog whose expression is strongly promoted by genotype background and photoperiod signalling, while *VRN-B1* provides additional adjustment to year-to-year environmental variation.

***VRN-B1* appears more environmentally responsive than *VRN-A1*.** For *VRN-B1*, genotype again con-

tributed strongly ( $P < 0.001^{***}$ ;  $R^2 = 0.258$ ), whereas tissue was not significant ( $P = 0.390$ ), indicating a weaker apex–leaf contrast than for *VRN-A1*, although leaf expression may still aid cold acclimation (Dhillon et al. 2010). Site showed a small but significant effect ( $P = 0.025^*$ ), and microclimate covariates (DL, GDD, TLS and FDS) were all highly significant ( $P < 0.001^{***}$ ), while interactions were not. In the reduced model, photoperiod class again affected *VRN-B1* ( $P < 0.001^{***}$ ;  $R^2 = 0.021$ ), with photoperiod-sensitive *ppd-D1b* genotypes showing

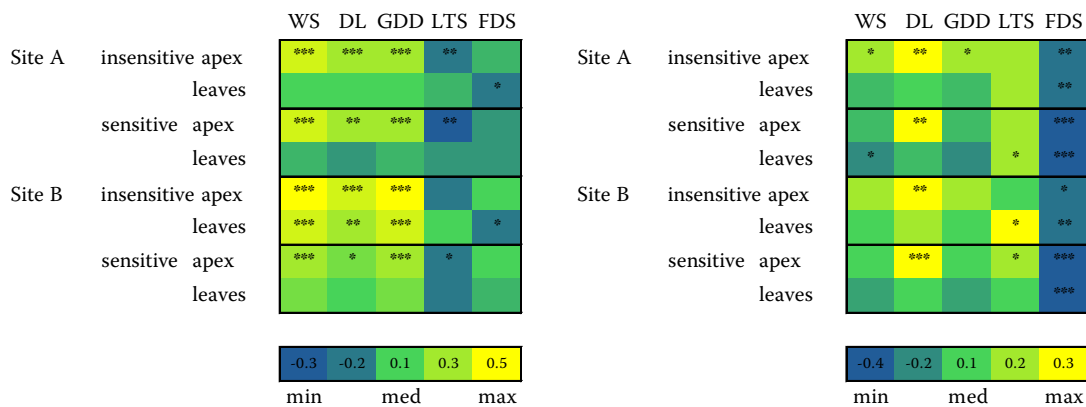


Figure 4. Spearman  $\rho$  heat maps (site  $\times$  type  $\times$  tissue): *VRN-A1* (A); *VRN-B1* (B)

WS – Waddington scale; DL – daylength; GDD – growing degree days; LTS – low temperature sum; FDS – freezing-degree sum; \*, \*\*, \*\*\*: significant at  $P < 0.05, 0.01, 0.001$

<https://doi.org/10.17221/76/2025-CJGPB>

higher *VRN-B1* expression than *Ppd-D1a* genotypes, in clear contrast to the *VRN-A1* pattern. Overall, *VRN-B1* was the homeolog most responsive to microclimate and temperature indices in our field data.

**Apex–leaf tissue specificity in *VRN-A1* responses.**

Across sites, tissues and photoperiod-sensitivity genotypes, Spearman analyses revealed few strong associations ( $P < 0.001$ ; Figure 4), all in the apex. At Site A, apex *VRN-A1* expression increased with apex developmental stage in both *Ppd-D1a* and *ppd-D1b* genotypes ( $\rho = 0.4$ ), and at the colder Site B photoperiod-insensitive *Ppd-D1a* genotypes also showed a positive association with GDD ( $\rho = 0.5$ ). In contrast, no  $P < 0.001$  correlations were detected for *VRN-A1* in leaves at Site B, underscoring clear tissue specificity. Apex *VRN-A1* follows gradual, cumulative activation with development and thermal time, whereas leaf *VRN-A1* appears more transient and closely tracks short-term low-temperature fluctuations. Together, these patterns support *VRN-A1* as a primarily apex-localised integrator of vernalisation and thermal time (Li & Dubcovsky 2015), with leaf expression remaining more dynamic and environmentally labile.

***VRN-B1* inversely associates with short-term freezing exposure across sites and tissues.** Across both sites and tissues, *VRN-B1* expression showed a consistent negative association with FDS (Spearman  $\rho = -0.3$  to  $-0.4$  in both *Ppd-D1a* and *ppd-D1b* genotypes). This inverse relationship suggests that short-term freezing exposure acts as a short-term “developmental brake”, with higher freezing load associated with lower *VRN-B1* and potentially slower apex progression during cold snaps, enhancing survival. Such plasticity is likely most relevant in photoperiod-sensitive genotypes, which progress later and retain greater scope for modulation, whereas earlier, photoperiod-insensitive lines may have less opportunity for this buffering.

## CONCLUSION

Under field conditions, *VRN-A1* might follow the developmental progression (apex > leaf) and seasonal forcing (day length, thermal time), whereas *VRN-B1* might be more responsive to short-term microclimate variation, including recent freezing-degree sum and small site differences. Photoperiod background further modulates timing; *Ppd-D1a* tends to advance development. Combining apex *VRN-A1* dynamics, *VRN-B1* sensitivity, and *Ppd-D1* group might guide

cultivar choice to site conditions. A key limitation is the comparison across diverse cultivars; targeted sequencing and near-isogenic line tests are needed to validate and further explain these field pattern.

**Acknowledgements.** The authors thank colleagues at the Field Experimental Station in Žabčice for cultivating the wheat and for technical support during sampling. The extended thanks go also the anonymous reviewers for their thoughtful comments and constructive suggestions, which substantially improved the clarity and scientific rigour of this manuscript.

## REFERENCES

- Aslam R., Williams L.E., Bhatti M.F., Virk N. (2017): Genome-wide analysis of wheat calcium ATPases and potential role of selected ACAs and ECAs in calcium stress. *BMC Plant Biology*, 17: 174.
- Beales J., Turner A., Griffiths S., Snape J.W., Laurie D.A. (2007): A pseudo-response regulator is misexpressed in the photoperiod insensitive *Ppd-D1a* mutant of wheat (*Triticum aestivum* L.). *Theoretical and Applied Genetics*, 115: 721–733.
- Brooking I. (1996): Temperature response of vernalization in wheat: A developmental analysis. *Annals of Botany*, 78: 507–512.
- Chen A., Dubcovsky J. (2012): Wheat TILLING mutants show that the vernalization gene *VRN1* down-regulates the flowering repressor *VRN2* in leaves but is not essential for flowering. *Plos Genetics*, 8: e1003134.
- Chen Y., Carver B.F., Wang S., Cao S., Yan L. (2010): Genetic regulation of developmental phases in winter wheat. *Molecular Breeding*, 26: 573–582.
- Curtis B.C., Rajaram S., Gómez Macpherson H. (2002): Bread Wheat: Improvement and Production. FAO. Available at <https://www.fao.org/3/y4011e/y4011e00.htm>
- Dhillon T., Pearce S.P., Stockinger E.J., Distelfeld A., Li C., Knox A.K., Vashegyi I., Vágújfalvi A., Galiba G., Dubcovsky J. (2010): Regulation of freezing tolerance and flowering in temperate cereals: The *VRN-1* connection. *Plant Physiology*, 153: 1846–1858.
- Distelfeld A., Tranquilli G., Li C., Yan L., Dubcovsky J. (2009): Genetic and molecular characterization of the *VRN2*/loci in tetraploid wheat. *Plant Physiology*, 149: 245–257.
- Frantová N. (2024): Winter wheat growth stages affecting the regulation of genes expression activated by abiotic stress [Dissertation Thesis.] Brno, Mendel University in Brno.
- Fu D., Szűcs P., Yan L., Helguera M., Skinner J.S., von Zitzewitz J., Hayes P.M., Dubcovsky J. (2005): Large deletions within the first intron in *VRN-1* are associated with spring

- growth habit in barley and wheat. *Molecular Genetics and Genomics*, 273: 54–65.
- Galiba G., Quarrie S.A., Sutka J., Morgounov A., Snape J.W. (1995): RFLP mapping of the vernalization (*Vrn1*) and frost resistance (*Fr1*) genes on chromosome 5A of wheat. *Theoretical and Applied Genetics*, 90: 1174–1179.
- Hemming M.N., Peacock W.J., Dennis E.S., Trevaskis B. (2008): Low-temperature and daylength cues are integrated to regulate FLOWERING LOCUS T in barley. *Plant Physiology*, 147: 355–366.
- Kamran A., Randhawa H.S., Yang R.-C., Spaner D. (2014): The effect of VRN1 genes on important agronomic traits in high-yielding Canadian soft white spring wheat. *Plant Breeding*, 133: 321–326.
- Khan A.R., Enjalbert J., Marsollier A.-C., Rousselet A., Goldringer I., Vitte C. (2013): Vernalization treatment induces site-specific DNA hypermethylation at the *VERNALIZATION-A1* (*VRN-A1*) locus in hexaploid winter wheat. *BMC Plant Biology*, 13: 209.
- Kiss T., Balla K., Veisz O., Láng L., Bedő Z., Griffiths S., Isaac P., Karsai I. (2014): Allele frequencies in the *VRN-A1*, *VRN-B1* and *VRN-D1* vernalization response and *PPD-B1* and *PPD-D1* photoperiod sensitivity genes, and their effects on heading in a diverse set of wheat cultivars (*Triticum aestivum* L.). *Molecular Breeding*, 34: 297–310.
- Košner J., Pánková K. (2002): Vernalization response of some winter wheat cultivars (*Triticum aestivum* L.). *Czech Journal of Genetics and Plant Breeding*, 38: 97–103.
- Langer S.M., Longin C.F.H., Würschum T. (2014): Flowering time control in European winter wheat. *Frontiers in Plant Science*, 5: 537.
- Li C., Dubcovsky J. (2008): Wheat FT protein regulates *VRN1* transcription through interactions with FDL2. *The Plant Journal*, 55: 543–554.
- Li C., Lin H., Dubcovsky J. (2015): Factorial combinations of protein interactions generate a multiplicity of florigen activation complexes in wheat and barley. *The Plant Journal*, 84: 70–82.
- Loukoianov A., Yan L., Blechl A., Sanchez A., Dubcovsky J. (2005): Regulation of *VRN-1* vernalization genes in normal and transgenic polyploid wheat. *Plant Physiology*, 138: 2364–2373.
- NOAA (2025): Global Monitoring Laboratory (GML). Solar Calculator. National Oceanic and Atmospheric Administration. Available at <https://gml.noaa.gov/grad/solcalc/> (accessed Sept 2, 2025).
- Oliver S.N., Finnegan E.J., Dennis E.S., Peacock W.J., Trevaskis B. (2009): Vernalization-induced flowering in cereals is associated with changes in histone methylation at the *VERNALIZATION1* gene. *Proceedings of The National Academy of Sciences*, 106: 8386–8391.
- Petr J., Hnilička F. (2002): Changes in requirements on vernalization of winter wheat varieties in the Czech Republic in 1950–2000. *Rostlinná výroba*, 48: 148–153.
- Pfaffl M.W. (2001): A new mathematical model for relative quantification in real-time RT-PCR. *Nucleic Acids Research*, 29: 45e–45.
- Prášil I.T., Musilová J., Prášilová P., Janáček J., Couřová M., Kosová K., Klíma M., Hermuth J., Holubec V., Vítámvás P. (2025): Effect of geographical origin, regional adaptation, genotype, and release year on winter hardiness of wheat and triticale accessions evaluated for six decades in trials. *Scientific Reports*, 15: 5961.
- Sehgal D., Dixon L., Pequeno D., Hyles J., Lacey I., Crossa J., Bentley A., Dreisigacker S. (2023): Genomic insights on global journeys of adaptive wheat genes that brought us to modern wheat. In: *Compendium of Plant Genomes*. Springer International Publishing: 213–239.
- Shcherban A.B., Börner A., Salina E.A. (2015): Effect of *VRN-1* and *PPD-D1* genes on heading time in European bread wheat cultivars. *Plant Breeding*, 134: 49–55.
- Slafer G.A., Casas A.M., Igartua E. (2023): Sense in sensitivity: difference in the meaning of photoperiod insensitivity between wheat and barley. *Journal of Experimental Botany*, 74: 3923–3932.
- Smaczniak C., Immink R.G.H., Angenent G.C., Kaufmann K. (2012): Developmental and evolutionary diversity of plant MADS-domain factors: Insights from recent studies. *Development*, 139: 3081–3098.
- Snape J.W., Butterworth K., Whitechurch E., Worland A.J. (2001): Waiting for fine times: Genetics of flowering time in wheat. *Euphytica*, 119: 185–190.
- Strejčková B., Mazzucotelli E., Čegan R., Milec Z., Brus J., Çakır E., Mastrangelo A.M., Özkan H., Šafář J. (2023): Wild emmer wheat, the progenitor of modern bread wheat, exhibits great diversity in the *VERNALIZATION1* gene. *Frontiers in Plant Science*, 13: 1106164.
- Stelmakh A.F. (1992): Genetic effects of *Vrn* genes on heading date and agronomic traits in bread wheat. *Euphytica*, 65: 53–60.
- Takatsuji H. (1998): Zinc-finger transcription factors in plants. *Cellular and Molecular Life Sciences*, 54: 582–596.
- Waddington S.R., Cartwright P.M., Wall P.C. (1983): A quantitative scale of spike initial and pistil development in barley and wheat. *Annals of Botany*, 51: 119–130.
- Wenda-Piesik A., Holková L., Solařová E., Pokorný R. (2016): Attributes of wheat cultivars for late autumn sowing in genes expression and field estimates. *European Journal of Agronomy*, 75: 42–49.
- Xu S., Chong K. (2018): Remembering winter through vernalisation. *Nature Plants*, 4: 997–1009.

<https://doi.org/10.17221/76/2025-CJGPB>

- Xu S., Dong Q., Deng M., Lin D., Xiao J., Cheng P., Xing L., Niu Y., Gao C., Zhang W., Xu Y., Chong K. (2021): The vernalization-induced long non-coding RNA VAS functions with the transcription factor TaRF2b to promote *TaVRN1* expression for flowering in hexaploid wheat. *Molecular Plant*, 14: 1525–1538.
- Yan L., Loukoianov A., Blechl A., Tranquilli G., Ramakrishna W., SanMiguel P., Bennetzen J.L., Echenique V., Dubcovsky J. (2004): The wheat *VRN2* gene is a flowering repressor down-regulated by vernalization. *Science*, 303: 1640–1644.
- Yan L., Fu D., Li C., Blechl A., Tranquilli G., Bonafede M., Sanchez A., Valarik M., Yasuda S., Dubcovsky J. (2006): The wheat and barley vernalization gene *VRN3* is an orthologue of FT. *Proceedings of The National Academy of Sciences*, 103: 19581–19586.
- Zhang H., Xue X., Guo J., Huang Y., Dai X., Li T., Hu J., Qu Y., Yu L., Mai C., Liu H., Yang L., Zhou Y., Li H. (2022): Association of the recessive allele *vrn-D1* with winter frost tolerance in bread wheat. *Frontiers in Plant Science*, 13: 879768.
- Zhang X.K., Xiao Y.G., Zhang Y., Xia X.C., Dubcovsky J., He Z.H. (2008): Allelic variation at the vernalization genes *Vrn-A1*, *Vrn-B1*, *Vrn-D1*, and *Vrn-B3* in Chinese wheat cultivars and their association with growth habit. *Crop Science*, 48: 458–470.

Received: September 2, 2025

Accepted: December 31, 2025

Published online: February 9, 2026